Video Article

Optical Quantification of Intracellular pH in *Drosophila melanogaster* Malpighian Tubule Epithelia with a Fluorescent Genetically-encoded pH Indicator

Adam J. Rossano[1], Michael F. Romero[1,2]

[1]Department of Physiology and Biomedical Engineering, Mayo Clinic College of Medicine

[2]Department of Nephrology and Hypertension, Mayo Clinic College of Medicine

Correspondence to: Adam J. Rossano at rossano.adam@gmail.com, Michael F. Romero at Romero.michael@mayo.edu

URL: https://www.jove.com/video/55698
DOI: doi:10.3791/55698

Keywords: Biochemistry, Issue 126, Ion transport, intracellular pH, epithelia, Malpighian tubules, *Drosophila*, fluorescent reporter, genetically encoded pH indicator, pH regulation, live imaging, pHerry

Date Published: 8/11/2017

Citation: Rossano, A.J., Romero, M.F. Optical Quantification of Intracellular pH in *Drosophila melanogaster* Malpighian Tubule Epithelia with a Fluorescent Genetically-encoded pH Indicator. *J. Vis. Exp.* (126), e55698, doi:10.3791/55698 (2017).

Abstract

Epithelial ion transport is vital to systemic ion homeostasis as well as maintenance of essential cellular electrochemical gradients. Intracellular pH (pH_i) is influenced by many ion transporters and thus monitoring pH_i is a useful tool for assessing transporter activity. Modern Genetically Encoded pH-Indicators (GEpHIs) provide optical quantification of pH_i in intact cells on a cellular and subcellular scale. This protocol describes real-time quantification of cellular pH_i regulation in Malpighian Tubules (MTs) of *Drosophila melanogaster* through *ex vivo* live-imaging of pHerry, a pseudo-ratiometric GEpHI with a pK_a well-suited to track pH changes in the cytosol. Extracted adult fly MTs are composed of morphologically and functionally distinct sections of single-cell layer epithelia, and can serve as an accessible and genetically tractable model for investigation of epithelial transport. GEpHIs offer several advantages over conventional pH-sensitive fluorescent dyes and ion-selective electrodes. GEpHIs can label distinct cell populations provided appropriate promoter elements are available. This labeling is particularly useful in *ex vivo*, *in vivo*, and *in situ* preparations, which are inherently heterogeneous. GEpHIs also permit quantification of pH_i in intact tissues over time without need for repeated dye treatment or tissue externalization. The primary drawback of current GEpHIs is the tendency to aggregate in cytosolic inclusions in response to tissue damage and construct over-expression. These shortcomings, their solutions, and the inherent advantages of GEpHIs are demonstrated in this protocol through assessment of basolateral proton (H^+) transport in functionally distinct principal and stellate cells of extracted fly MTs. The techniques and analysis described are readily adaptable to a wide variety of vertebrate and invertebrate preparations, and the sophistication of the assay can be scaled from teaching labs to intricate determination of ion flux via specific transporters.

Video Link

The video component of this article can be found at https://www.jove.com/video/55698/

Introduction

The goal of this protocol is to describe quantification of intracellular pH (pH_i) using a Genetically-Encoded pH-Indicator (GEpHI) and demonstrate how this method can be used to assess basolateral H^+ transport in a model insect (*D. melanogaster*) renal structure, the Malpighian tubule (MT). MTs serve as the excretory organs of the fruit fly and are functionally similar to the mammalian nephron in several key respects[1]. MTs are arranged as 2 pairs of tubules (anterior and posterior) in the thorax and abdomen of the fly. The single-cell epithelial tube of each MT is composed of metabolically active principal cells with distinct apical (luminal) and basolateral (hemocoel) polarity as well as intercalated stellate cells. Anterior MTs are composed of 3 morphologically, functionally, and developmentally distinct segments, notably the initial dilated segment, transitional segment, and secretory main segment, which joins to the ureter[2]. At the cellular scale trans-epithelial ion transport into the lumen is accomplished by an apical plasma membrane V-ATPase[3] and an alkali-metal/H^+ exchanger as well as a basolateral Na^+-K^+-ATPase[4], inward-rectifier K^+ channels[5], Na^+-driven Cl^-/HCO_3^- exchanger (NDAE1)[6], and Na^+-K^+-$2Cl^-$ cotransporter (NKCC; Ncc69)[7], while stellate cells mediate Cl^- and water transport[8,9]. This complex but accessible physiologic system provides excellent opportunities for investigation of endogenous ion transport mechanisms when combined with the diverse genetic and behavioral toolsets of *Drosophila*.

The rationale for this protocol was to describe a genetically malleable system for studying epithelial ion transport with potential for integration from cell to behavior and export of tools to other model systems. Expression of pHerry[10], a GEpHI derived from a fusion of green pH-sensitive super-ecliptic pHluorin[11,12] (SEpH) and red pH-insensitive mCherry[13], in MTs permits quantification of H^+ transport in single MT cells through the high K^+/nigericin calibration technique[14]. As many ion transporters move H^+ equivalents, quantification of intracellular pH_i serves as a functional representation of ion movement via a variety of transporters. The *Drosophila* MT model system also offers powerful genetic tools in tissue-specific transgene[15] and RNA interference (RNAi)[16] expression, which can be combined with cellular imaging and whole-organ assays[17,18,19] of tubule function to create a robust toolset with vertical integration from molecules to behavior. This stands in contrast to many other protocols for assessing epithelial biology, as historically such measurements have relied on intricate and daunting micro-dissection, sophisticated ion-selective electrodes[20,21], and expensive pH-sensitive dyes[22] with restrictive loading requirements and poor cellular specificity in heterogeneous

tissues. GEpHIs have been used to extensively measure pH_i in a variety of cell types[23]. Early work exploited the inherent pH-sensitivity of Green Fluorescent Protein (GFP) to monitor pH_i in cultured epithelial cells[24] but the past two decades have seen GEpHIs used in neurons[25], glia[26], fungi[27], and plant cells[28]. The combination of the potential for cellular targeting of genetic constructs through the GAL4/UAS expression system[15] and the physiologic accessibility of the *Drosophila* MT make this an ideal preparation for investigations of pH_i regulation and epithelial ion transport.

pH_i regulation has been studied for decades and is vital to life. The MT preparation offers a robust model to teach physiology of pH_i regulation but also perform sophisticated investigations of pH_i regulation *ex vivo* and *in vivo*. This protocol describes quantification of H^+ movement across the basolateral membrane of the epithelial cells of the *Drosophila* MT using the NH_4Cl pulse acid loading technique[21], but as the pH-indicator is genetically encoded, these methods and their theoretical framework can be applied to any preparation amenable to transgenesis and live-imaging.

Protocol

All steps in this protocol comply with the Mayo Clinic (Rochester, MN) animal use guidelines.

1. Fly Husbandry

1. Raise flies and set crosses according to standard husbandry[29].
   NOTE: Fluorescent reporter expression by the GAL4/UAS system is proportional to temperature and thus rearing temperature can be adjusted to alter expression level. While high expression levels often lead to a better signal-to-noise ratio this condition is also associated with increased cytosolic and organellar aggregates when using GFP to Red Fluorescent Protein (RFP) fusion constructs such as pHerry[10,30,31]. If aggregation is unavoidable, quantification is still possible by performing point calibrations in each experiment and normalizing data such that a fluorescence ratio of 1.0 corresponds to pH_i 7.0 (see step 7.4 Note on calibration below).
2. Set crosses of homozygous *capaR-GAL4*[32] males to homozygous *UAS-pHerry*[10] virgin females and homozygous *c724-GAL4*[2] males to homozygous *UAS-pHerry* virgin females to permit imaging of pH_i in principal cells and stellate cells of the MT, respectively. Place 6 UAS-pHerry females with 3 GAL4 males into fresh vials of food and leave to mate at 28 °C.
   NOTE: Larvae should be evident within 4 d and adults will begin to eclose around day 10.
3. Collect female flies upon eclosion and set aside to age for 10 d at 28 °C.
   NOTE: The timing of experimentation can be adjusted to correspond to any restrictive behavioral assays (such as the Ramsay secretion assay[17,19]) that will be correlated to intracellular live pH imaging. Male flies can be used but tubules from females are often larger and more robust.

2. Preparation of Poly-L-Lysine Slides.

1. Draw a 40 x 20 mm border with a hydrophobic PAP pen around the top of standard 75 x 25 mm slides and set aside to dry for 15 min at RT. Use large coverslips if the slides are not compatible with imaging optics.
2. Transfer 2 mL of stock 0.01% Poly-L-Lysine (PLL) solution onto each slide and set aside for 1 h at RT.
3. Remove excess PLL with a pipette. Save the solution in a 50 mL conical vial for future use. Store at 4 °C.
4. Aspirate any remaining solution with a vacuum line. Run the vacuum line over the entire slide surface to ensure that no solution remains on the slides.
5. Set the slides aside for 1 additional h at RT prior to use. Store the slides dry at RT for up to 1 month in a standard slide book.

3. Preparation of Dissecting Dish and Glass Rods

1. Add 0.5 mL of elastomer curing agent to 4.5 mL of elastomer base in a 35 x 10 mm polystyrene Petri dish at RT to produce a depth of 5 mm. Mix with a disposable pipette tip. Allow elastomer to cure O/N at RT.
   NOTE: Elastomer should be clear and free of bubbles. Clearing of bubbles may be facilitated by keeping elastomer plates in a vacuum jar for 10 - 15 min after pouring.
2. Hold a 5 mm diameter glass rod between hands and melt the center of the rod over a lit Bunsen burner while pulling the ends apart. As the glass melts pull more quickly to produce a thin (0.1 mm) and tapered shaft (**Figure 1**).
   NOTE: A 45 ° angle at the shank is often helpful in handling tubules. This can be achieved by lowering one hand as the shank is pulled (see **Figure 1**).
3. Break the thin shaft in the middle with the blunt side of a single-edged carbon steel razor blade. Inspect the thin end of the rod under a dissecting scope to ensure the break is clean.

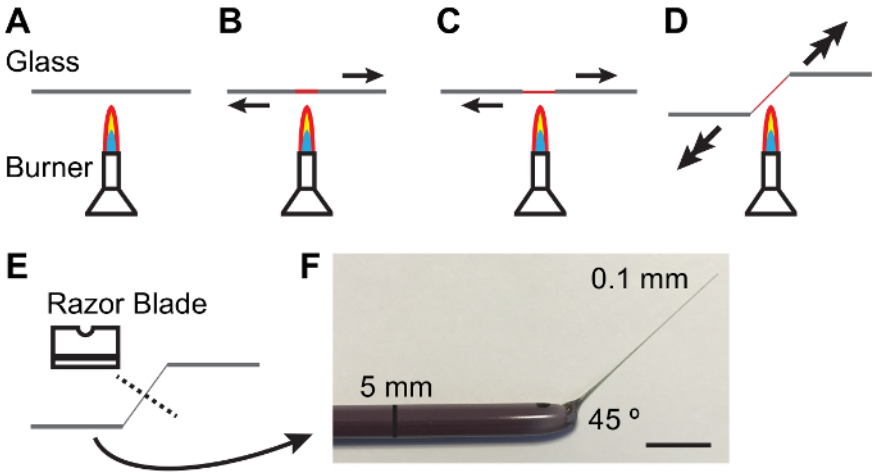

Figure 1: Fabricating Glass Rods for Handling Malpighian Tubules.
A - E. Process of heating and pulling a glass rod to produce a taper and angle suitable for handling MTs. Arrows denote direction and magnitude of force to be applied. **F**. Photograph of an appropriately fabricated glass tool. Scale bar = 10 mm. Please click here to view a larger version of this figure.

4. Preparation of Solutions and Perfusion System

NOTE: Perfusion systems differ by manufacturer. This protocol is based around a gravity-fed 8-channel open reservoir with an input flow rate regulator and a vacuum-driven outflow, but the method of mounting MTs as described here can be adapted to work with any perfusion system.

1. **Prepare the following solutions:**
    1. Aliquot Schneider's medium (40 mL into 50 mL conical vials) and store at 4 °C.
    2. Prepare solutions (*i.e.* insect Phosphate-Buffered Saline (iPBS) and iPBS with NH_4Cl) at RT as needed according to **Table 1**). Warm solutions to RT before use on day of experiment.
    NOTE: iPBS and iPBS with 40 mM NH_4Cl can be prepared in large volumes (1 L or more) and stored at 4 °C.
    3. Prepare 8 calibration solutions in 500 mL volumes at pH = 5.0, 6.0, 6.5, 7.0, 7.3, 7.6, 8.0, and 9.0 as indicated in **Table 1** and store at 4 °C. Adjust pH of each solution by titration with N-methyl-D-glucamine (NMDG) and HCl.
    4. On the day of experiments, warm 5 mL aliquots of calibration solutions to RT and add stock nigericin solution (20 mM in dimethyl sulfoxide (DMSO)) to produce a final concentration of 10 µM.
    CAUTION: Handle nigericin with gloves. Treat all equipment that comes in contact with nigericin as disposable. Nigericin remains on glass and plastic and will compromise biological preparations if equipment is reused.

2. **Perfusion system:**
    1. Prime the perfusion system by filling all reservoirs with ddH_2O (**Figure 2**). Open the channels one at a time to allow all lines proximal to the flow rate regulator to fill.
    NOTE: It may be necessary to clear air in the lines by opening the stalled channel and using a plunger to drive flow from the reservoir.
    2. Open 2 channels and allow ddH_2O to drain. Once the reservoirs are nearly empty, fill the first reservoir with iPBS and the second reservoir with NH_4Cl-pulsed iPBS. Set flow rate to maximum with the flow rate regulator and allow each solution to flow for 1 min to fill the distal lines, then stop the flow (**Figure 2**).
    3. Position 2 sets of soldering "helping hands" clamps on the imaging microscope stage. Place one clamp on each side of the imaging platform.
    4. Carefully heat the distal 0.5 inches of a piece of capillary glass (inner diameter 1.5 mm, outer diameter 0.86 mm, length 100 mm) over a Bunsen burner. Create a 45 ° bend by allowing the distal end to bend by gravity and removing the glass from the flame once the desired angle is achieved. Repeat this process with a second piece of capillary glass.
    5. Insert the bent glass capillaries in the in-flow line and vacuum-connected outflow line, respectively and mount them in the "helping hands" to align them with the imaging stage of the microscope (**Figure 3**).

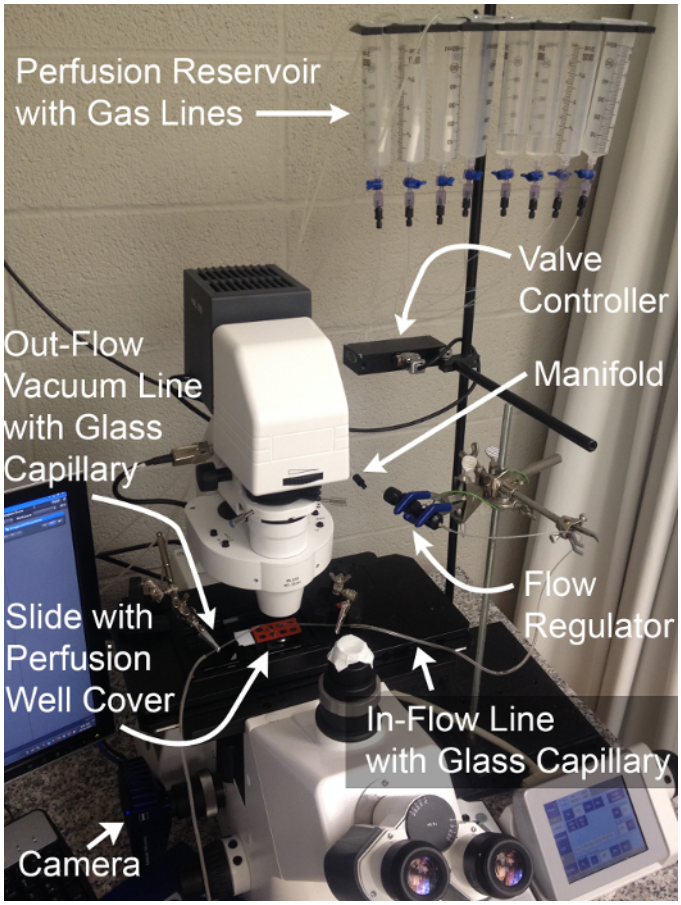

Figure 2: Perfusion System and Imaging Configuration.
Components necessary for the physiological assessment of MT basolateral transport function through simultaneous live fluorescence imaging and rapid solution exchange.Gas lines shown are optional and permit expansion of experiments to the assessment of HCO_3^- transport. Please click here to view a larger version of this figure.

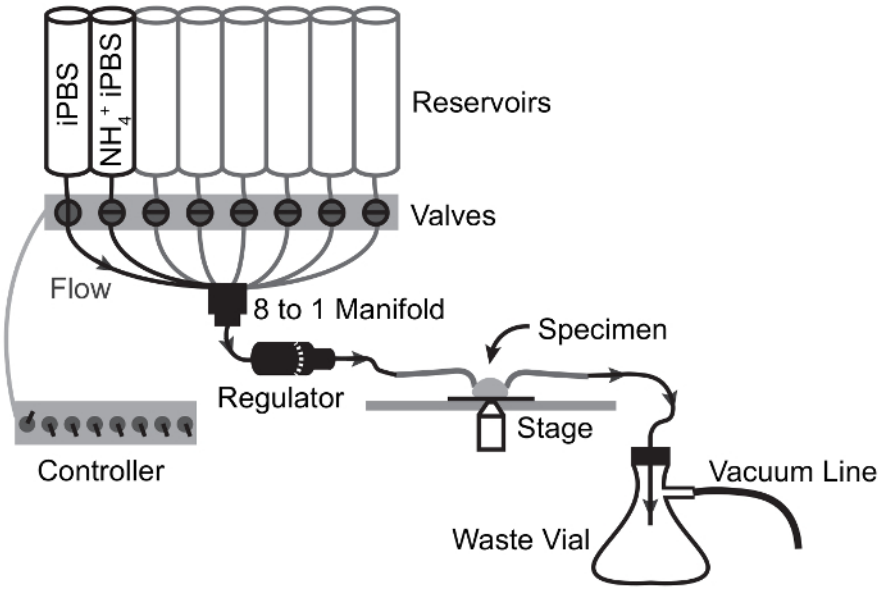

Figure 3: Flow Schematic of Perfusion Apparatus for NH_4Cl Pulse Experiments.
Arrows depict flow path and valve switching points. Solution moves from reservoir to specimen by gravity flow and is drawn from the specimen chamber to the waste flask by vacuum suction. Please click here to view a larger version of this figure.

5. Dissection of Adult *Drosophila* Anterior Malpighian Tubules.

1. Gather the dissection dish and pulled glass rod from section 3, a PLL-coated slide from section 2, an adhesive perfusion-well divider, vacuum grease, a 4 x 2" strip of sealing film, 2 pairs of #5 fine forceps, and 40 mL aliquots of ice-cold Schneider's medium and RT iPBS.
2. Spread vacuum grease on the sealing tape and press the adhesive perfusion-well divider onto the tape to coat the bottom with grease. Peel off the adhesive perfusion-well divider and place it grease-side-down on top of a PLL coated slide. Remove the perfusion-well divider to leave individual specimen wells traced in hydrophobic grease.
3. Place 200 µL of RT iPBS in the grease-encircled well on the PLL coated slide and move the slide under the stereoscope.
4. Place *UAS-pHerry/capaR-GAL4* flies in an empty fly vial and anesthetize them on ice for 10 min.
   NOTE: This method of anesthesia, unlike CO_2, ensures that the flies do not dehydrate.
5. Pour ice-cold Schneider's medium into the dissecting dish and use fine forceps to transfer a single anesthetized female fly into the dish under a dissecting stereoscope.
6. Hold the fly by the thorax with a set of forceps and use the other to gently grip the posterior of the abdomen. Pull open the posterior of the fly using the forceps in short, deliberate motions. Once the hindgut is visible, grip the distal end and free the gut and MTs from the underlying tracheoles by pulling the hindgut away from the body through repetitive, brief tugs.
   NOTE: The anterior and posterior MTs will be visible where they meet the junction of the midgut and hindgut through the ureter. The first pair of MTs to be free will likely be the posterior tubules as they encircle the hindgut. These can be ignored (**Figure 4A**).
7. Pinch off the anterior MTs at the ureter with fine forceps once the second set of MTs is free of the abdomen. This will separate the anterior MTs from the gut and close the ureter.
8. Pick up the free anterior MTs with the pulled glass rod by sliding the rod under the ureter such that the tubules fall to either side. Lift the MTs straight up out of the solution.
9. Turn the glass rod such that the MTs and ureter are adhered to the underside of the rod and lower the ureter straight down onto the slide. Affix the ureter and seal the distal ends of the MTs by pressing the ureter down onto the glass slide (**Figure 4B**). Do not manipulate the MTs any more than necessary. The MTs should be floating up in the solution with the ureter anchored to the slide.
10. Use the fine end of the glass rod to gently sweep each tubule across the slide surface. Brace the rod against the slide to avoid crushing the tubule and slide the rod over the top of the tubule, moving distal to proximal, to attach the full length of each tubule to the surface of the PLL-coated slide (**Figure 4C**).
11. Place the adhesive perfusion-well divider back on the slide to form a small fluid-filled well over the mounted tubule.
12. Place the specimen on the microscope stage. Position the inflow and outflow capillaries over the inlet and outlet opening of the perfusion well, respectively.
    NOTE: The well divider can be left off if an open perfusion chamber is desired. In this case the inflow and outflow capillaries can be aligned to opposite sides of an imaging well.

6. Validation of Imaging Protocol and Tubule Health

Note: This protocol is performed on an inverted wide-field epifluorescent microscope with GFP (SEpH) and RFP (mCherry) filter sets (470/40 nm excitation (ex), 515 nm longpass emission (em), 500 nm dichroic and 546/10 nm ex, 590 nm longpass em, 565 nm dichroic), a 10X/0.45 air objective, a monochromatic camera for live-image capture, and imaging software. The protocol can be adapted for any upright or inverted microscope with automated filter switching between GFP and RFP optics and image acquisition software, although optimal exposure times, light intensity, and binning parameters will vary. In all analysis, the fluorescence intensity should be analyzed as mean pixel intensity in the region of interest (ROI), after background subtraction in each channel using an ROI with contains no fluorescence adjacent to the signal ROI.

1. Turn on the microscope, light source, and imaging system.
2. Open associated imaging software.
3. Look through the eyepiece and manually adjust focus until the lumen of the MT is clearly visible under transmitted light.
4. Click the "Acquisition" tab in image analysis software and select "2x2" in the "Binning" pull-down menu in the "Acquisition Mode" section.
5. Insert a 5% neutral density filter into the light path to reduce illumination light and minimize photobleaching.
6. Click the GFP (SEpH) channel in the "Channels" menu, then click "Live" to observe the fluorescent signal via the camera.
7. Adjust the "Time" slider to set the exposure time such that the brightest pixel values in the intensity histogram are approximately 40% of the maximum value, then click "Stop" to stop the illumination.
8. Repeat steps 6.6 - 6.7 in the RFP (mCherry) channel and confirm the presence of the dilated initial segment of the anterior MT and the absence of cytosolic mCherry aggregates (indicative of tissue damage or overexpression) (**Figure 4D**).
   NOTE: The dilated segment should be clearly apparent as it is the most proximal segment of the tubule and the diameter of the inner lumen of this segment is ~20 µm greater than that of the adjacent transitional segment. 2 x 2 pixel binning is often sufficient but can be increased to further reduce the required illumination intensity. Typical exposure times are between 150 & 800 ms/channel. Use as little light as possible to minimize photobleaching. Minimizing photobleaching is vital to the use of dual-fluorophore indicators such as pHerry as the two fluorophores can bleach independently, thus invalidating any ratio calibration.
9. Enable a time-lapse imaging protocol by clicking the "Time Series" check box.
10. Adjust the "Duration" in the pull-down menu in the "Time Series" section to 10 min and the "Interval" slider to 0 to set the total capture time with a maximum image acquisition rate. A total acquisition rate of 0.2 Hz is often sufficient.
11. Check both the GFP (SEpH) and RFP (mCherry) boxes in the "Channels" section.
12. Open the iPBS line of the perfusion system by activating the appropriate valve controller and start the imaging protocol by clicking "Start Experiment." After 1 min, switch to NH_4Cl pulse solution for 20 s by opening the appropriate valve and closing the iPBS line, then return to iPBS by closing the NH_4Cl line and reopening the iPBS valve. Allow the full imaging protocol to complete before stopping the perfusion system.
    NOTE: Time-lapse analysis should reveal a stable mCherry signal and a SEpH signal which increases in the presence of NH_4Cl, quenches upon washout, and gradually recovers.
13. Perform a 2-point calibration.

1. Remove the well divider by peeling it away from the underlying slide and remove the perfusion capillaries and clamps from the imaging well.
2. Apply 200 µL Calibration iPBS (pH 7.4, 10 µM nigericin) to the imaging well with a 200 µL pipette. Remove the solution from the imaging well with the pipette, then replace with another 200 µL of calibration solution. Repeat this process 4 times to ensure complete solution exchange.
3. Incubate the preparation in calibration solution for 30 min before imaging. Repeat the imaging protocol using the same parameters determined in steps 6.6 - 6.11, with the modification of only 1 min of image capture.
   NOTE: The perfusion system and capillaries are not needed in this step and should not be attached to the imaging well to avoid exposing the capillaries to nigericin.
4. Add 200 µL Calibration iPBS (pH 9.0, 10 µM nigericin) to the imaging well with a 200 µL pipette. Remove the solution from the imaging well with the pipette, then replace with another 200 µL of calibration solution. Repeat this process 4 times to ensure complete solution exchange.
5. Incubate the preparation in the second calibration solution for 10 min before imaging. Repeat the imaging protocol as in step 6.13.3.
6. Review the captured image stack in image analysis software to confirm that no pixels in either channel are saturated by clicking "Mean ROI" and scrolling though the image stack with the "Frame" slider while observing that no values reported in the intensity histogram reach the maximum detectable value. If any frames contain pixels that reach the maximum detectable intensity, reduce the exposure time or illumination intensity and repeat section 6.
   Note: Once established do not change imaging parameters between experiments or calibration unless point calibrations are to be used in each preparation (see step 8.3).

14. Analyze the image stack to plot fluorescent intensity and fluorescence ratio (SEpH/mCherry) as a function of time.
    1. Click "Mean ROI" and select the freeform tool. Hold left-click to trace a ~50 µm length of MT. Right click to finish drawing the ROI, then repeat in an area adjacent to the MT to define a background ROI (**Figure 5A**).
    2. Click "Mean Intensity" under "Measurements." Create a table of intensity values by clicking "Export > Data Table > Create."
    3. Click the configuration cogwheel icon and de-select all parameters except "Time" and "Mean Intensity." Right-click the tab for the newly created data table, select "Save As", and export the data as a .csv file.
       NOTE: Similar measurements can also be made using free software such as ImageJ.
    4. Open a spreadsheet table and import the data table by selecting the "Data" tab followed by "From Text".
    5. Use functions in the spreadsheet to subtract the SEpH Background Intensity from the SEpH Signal Intensity at each time point. Repeat this process for the mCherry signal.
    6. Plot each channel intensity as a function of time by selecting the columns containing the Time and background-corrected Intensity data and then clicking "Insert > Scatter (Charts) > Scatter with Straight Lines" (**Figure 5B**).
    7. Use spreadsheet functions to calculate the SEpH/mCherry fluorescence ratio at each time point.
    8. Plot fluorescence ratio as a function of time by selecting the columns containing the Time and ratio data and then clicking "Insert > Scatter (Charts) > Scatter with Straight Lines" (**Figure 5C**).

7. Full Calibration of pHerry in Malpighian Tubules *Ex Vivo*.

1. Dissect and mount a fresh set of anterior MTs as described in section 5.
2. Exchange iPBS for Calibration iPBS (pH 7.4, 10 µM nigericin) as described in step 6.13.2. Incubate for 30 min.
3. Locate the MTs and collect pairs of SEpH/mCherry images as described in steps 6.1 - 6.11. Replace the solution with another stock of Calibration iPBS as described in step 6.13.4, wait 10 min, and image again. Repeat this process until the SEpH/mCherry ratio has been imaged in all solutions. Obtain pH 9.0 images last as the specimen rarely recovers from high pH.
4. Plot fluorescence ratio of SEpH to mCherry from calibrations in eight specimens as a function of imposed pH_i as described in step 6.14.9. Fit the calibration data with a Boltzmann curve to obtain full calibration function according to Equation 1 (**Figure 5D**). If data are inconsistent, plot calibration sets from each specimen normalized such that a fluorescence ratio of 1.0 corresponds to pH_i 7.0 and re-analyze (**Figure 5E**).
   NOTE: If the latter process is necessary individual experiments will need their own internal point calibrations[33] (see quantification procedure below (step 8.3)).
5. **Equation 1**

$$R = \left(\frac{A_1 - A_2}{1 + e^{(pH_i - x_o)/dx}}\right) + A_2$$

Where R = SEpH/mCherry ratio and A_1, A_2, x_o, and dx are curve fitting parameters representing minimum fluorescence ratio, maximum fluorescence ratio, pK_a, and width of the function respectively. x_o = apparent pK_a of pHerry, which can vary between 7.1 and 7.4 depending on the cell type and exact calibration conditions.

8. Quantification of Basolateral Acid Extrusion from *Ex Vivo* Malpighian Tubule Epithelia.

1. Image pHerry-expressing stellate cells and pHerry-expressing principal cells simultaneously.
   1. Dissect anterior MTs from a *UAS-pHerry/capaR-GAL4* fly as described in section 5, but do not transfer MTs from the dissecting Schneider's medium to the imaging well.
   2. Dissect anterior MTs from a *UAS-pHerry/c724-GAL4* fly in the same dissecting dish using the procedure outlined in section 5.
   3. Transfer the 2 sets of MTs into the same imaging well as described in steps 5.8 - 5.11.
      NOTE: When sweeping the arms of the MTs down to the slide, place the MTs of the *UAS-pHerry/c724-GAL4* and the *UAS-pHerry/capaR-GAL4* tubules near each other so pHerry-expressing principal and stellate cells can be visualized in the same field (**Figure 6A**).

2. Apply the NH_4Cl prepulse as described in step 6.12.

NOTE: If consistent calibration (**Figure 4B**) could not be achieved, perform a point calibration by setting pH_i to 7.0 at the end of each experiment with Calibration iPBS (pH 7.0, 10 µM nigericin, 30 min incubation) after the adhesive perfusion-well divider and the perfusion equipment have been removed.

3. Calibrate traces from stellate and principal cells of different MT segments (using the absolute or normalized ratio as appropriate) with Equation 2 and analyze the recovery phase after NH_4Cl withdrawal by applying exponential decay functions using statistical analysis software and noting the decay constant (τ) (**Figure 6B**).

Equation 2

$$pH_i = \left(dx \times \ln\left(\frac{A_1 - A_2}{R - A_2} - 1\right)\right) + x_o$$

Where R = SEpH/mCherry ratio and A_1, A_2, x_o, and dx are curve fitting parameters determined by calibration in step 7.4 (**Equation 1**).

1. Calculate acid extrusion rate (J_{H+}, see **Equation 3**) as a function of pH_i to account for variations in resting pH_i and acid loading between preparations[34]. Use the exponential functions derived in step 8.3 to calculate the derivative of pH_i with regard to time in each time interval.

Equation 3

$$\text{Acid Extrusion Rate } (J_{H+}) = \beta_T \times \frac{dpH_i}{dt}$$

2. Calculate the intrinsic buffering capacity (β_i; **Equation 4**) of the cytosol at the pH_i from the start of each interval in step 8.3.1 based on previous literature (see **Equation 4**).
NOTE: In *Drosophila*, the most thorough characterization of β_i comes from larval motor nerve terminals[35] and these data can be assumed to hold for MT cells in the absence of other available data.

Equation 4

$$\beta_i = (-26.53 \times pH_i) + 205.65$$

3. Calculate the product of β_T (from step 8.3.2)$_{and}$ dpH_i/dt (from step 8.3.1) to determine J_{H+} (**Equation 3**).
NOTE: In nominally bicarbonate-free solutions such as those described in this protocol, bicarbonate-derived buffering capacity (β_b) is assumed to be ~0 mM. Total buffering capacity (β_T) is the sum of β_i and$_{\beta b}$, and thus $\beta_i = \beta_T$ in the absence of HCO_3^-/CO_2[36].
4. Plot J_{H+} as a function of the pH_i at the beginning of each time interval as outlined in step 6.14.9.
5. Apply exponential decay functions to the portion of all datasets which overlap in pH_i using statistical analysis software. Compare rates of change of the resulting functions to compare acid extrusion rates between cells and MT segments (**Figure 6C**).
NOTE: The most appropriate function used for curve fitting may not always be a single exponential. Other functions can be substituted if they improve the goodness of fit.
6. Calculate acid flux (see **Equation 5**) as a function of pH_i to account for variations in cell size and shape.

Equation 5

$$\text{Acid Flux} = J_{H+} \times \frac{\text{Cell Volume}}{\text{Cell Surface Area}}$$

NOTE: Cell dimensions can either be measured directly in images or approximated. Principal cells can be represented as halves of a hollow tube with the following dimensions: inner diameter 24 µm; outer diameter 48 µm; height 50 µm. Transitional stellate cells are variable but can be roughly represented as cylinders with heights of 50 µm and diameters of 10 µm. See final paragraph of **Representative Results** below.
7. Apply exponential decay functions to the portion of all datasets that overlap in pH_i using statistical analysis software. Compare rates of change of the resulting functions to compare acid fluxes between cells and MT segments (**Figure 6D**).

Representative Results

Healthy tissues and proper identification of anterior MTs are vital to the success of this protocol. During dissection, care should be taken to not directly touch the MTs and to only handle them by the ureter as gripping the MTs directly will lead to breakage (**Figure 4A - B**). When MTs are swept flat onto the slide, the tubules must be touched as little as possible and excess motion avoided as this will damage the single-cell epithelial layer (**Figure 4C**). Properly dissected anterior MTs will show even distribution of both red and green fluorescence through the cytosol of epithelial cells and morphologically distinct tubule segments. Tubules damaged by improper perfusion or mishandling will display aggregation of red fluorescence with no paired green aggregates, and misidentified posterior MTs will show uniform morphology from the proximal blind end to the distal ureter (**Figure 4D**).

Proper function of pHerry must be confirmed though physiologic assessment as well as morphology. The most expedient method of confirming proper pH-sensing is to apply an NH_4Cl pulse. Under these conditions the green SEpH signal should report the expected pH changes (a rise in pH_i during the pulse as NH_3 enters the cell, a gradual decline during the pulse as NH_4^+ enters through K^+ transporters and channels, and a rapid acidification and gradual recovery upon NH_4Cl withdrawal[21], while the red mCherry signal should remain constant (**Figure 5A - B**). The magnitude of changes in the SEpH signal will vary with protocol and cell type, but the mCherry signal should be stable in all cases. Changes in the mCherry signal during individual experiments indicate movement artifacts or progressive generation of sensor aggregates due to cell damage. The latter will prevent quantification of pH_i and must be avoided. Upon completing the NH_4Cl pulse it is important to perform a 2-point calibration (Calibration iPBS, pH 7.4 and 9.0, 10 µM nigericin) to confirm a resting pH_i near 7.4 and ensure that the current imaging parameters do not lead to saturation of fluorescence detection when fluorescence is maximized at pH 9.0 (**Figure 5C**). If resting pH is significantly lower than 7.4, the protocol should be repeated with healthy MTs; and if saturation occurs at pH 9.0, the protocol should be repeated with lower light intensity or exposure time. Once adequate imaging parameters are determined, they should not be changed between experiments or calibrations if the absolute fluorescence ratios are to be used. While the pseudo-ratiometric nature of pHerry can provide a method of movement correction in preparations prone to movement or changes in cell diameter, the absolute quantification of pH_i requires full systematic correlation of the pHerry SEpH/mCherry ratio to pH_i through the nigericin/high K^+ technique. The calibration of pHerry in healthy preparations should produce consistent calibration curves with an apparent pK_a of 7.1-7.4 depending on the cell type and calibration conditions (**Figure 5D**). For preparations in which mCherry aggregation is unavoidable, normalization of ratio values such that a fluorescence ratio of 1.0 corresponds to pH_i 7.0 should yield similar results (**Figure 5E**). If point calibrations and normalized curves are used, imaging parameters can be optimized for each preparation.

Calibrated pH_i traces can be used to compare pH regulatory mechanism between cell types. The GAL4/UAS expression system in *Drosophila* can be used to express pHerry in principal cells and stellate cells of the anterior MT (**Figure 6A**). pH_i regulation can be assessed by acid-loading cells with NH_4Cl pulses and quantifying the rate of pH_i recovery. This can be accomplished by fitting exponential functions to the recovery phase in different experimental conditions to extract the decay constant (τ) as cells with more rapid H^+ efflux will display a more rapid recovery (and thus lower values of τ). Based on this analysis, stellate cells of the MT appear to have more robust acid extrusion than principal cells (**Figure 6B**). This analysis will hold as long as the resting pH_i, extent of acid loading, and buffering capacity are similar between experimental groups. However, when these conditions are not met, it is necessary to account for the observation that intrinsic buffering capacity of the cytosol (β_i) of many cells is itself pH-dependent[35,37,38] and thus the rate of pH_i change at different pH_i may not be directly comparable. In such cases, exponential curves fit to the acid extrusion phase following an NH_4Cl pulse and previously determined estimates of intrinsic buffering capacity (β_i) can be used to plot the acid extrusion rate (J_{H+}) as a function of pH_i and determine compensated rate of acid extrusion (**Equations 3** & **4**). Once differences in acid loading and resting pH_i are accounted for, it is evident acid extrusion in principal cells of the transitional segment exceed that of stellate cells (**Figure 6C**). While compelling, this analysis does not address that measured pH_i is a function of volume while acid extrusion across the plasma membrane is a function of membrane surface area. Dividing J_{H+} by the surface area to volume ratio of the cell of interest will yield values in moles of acid equivalents per unit surface area per unit time (**Equation 5**), thus allowing correction for differences in cell size and morphology. Approximately two principal cells comprise the circumference of the MT in the transitional segments and thus single cells can be modelled as half of a tube (inner diameter 24 µm; outer diameter 48 µm; height 50 µm). Stellate cells are smaller and tend to be bar-shaped in the transitional segment of the MT[2]. Exact quantification of surface area and volume is difficult but even conservative approximations of transitional stellate cell shape (cylinder with a height of 50 µm and a diameter of 10 µm) indicate a surface area to volume ratio at least 2x that of principal cells. Taking this into account reveals that the stellate cell acid flux is significantly below that of transitional principal cells, and in fact approaches that of initial segment principal cells (**Figure 6D**).

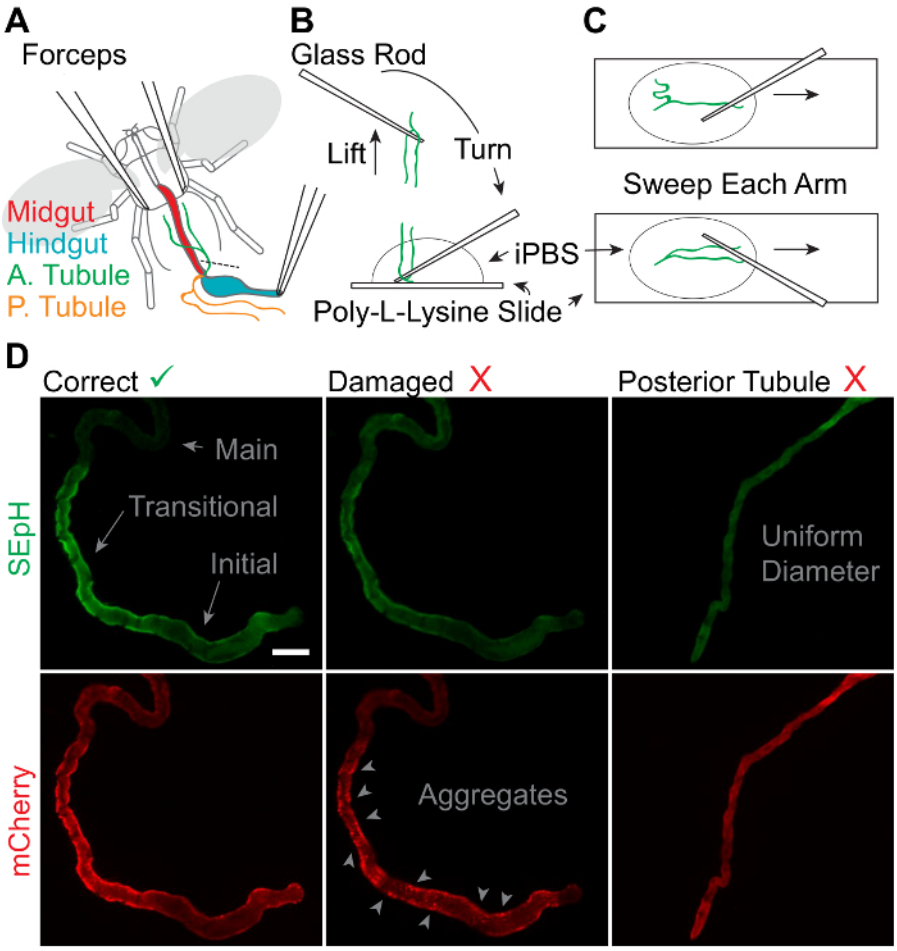

Figure 4: Dissection of Adult *Drosophila* Anterior Malpighian Tubules.
A. Schematic representation of anterior MT removal with 2 pairs of fine forceps in chilled Schneider's medium. "A. Tubule" = Anterior MT. "P. Tubule" = posterior MT. **B**. Process of retrieving and mounting extracted MTs using thin glass rods. **C**. Process of adhering the full length of extracted MTs to a slide for imaging and physiologic assessment. **D**. Representative widefield images of the SEpH (470/510 nm ex/em) and mCherry (556/630 nm ex/em) components of *UAS-pHerry* driven by *capaR-GAL4* depicting healthy anterior MTs, anterior MTs damaged by insufficient perfusion, and misidentified posterior MTs. Note that healthy anterior MTs display a clear dilated blind initial segment, a constricted transitional segment with relatively increased expression of *UAS-pHerry* when driven by *capaR-GAL4*, and a distal main segment. Damaged MTs display noticeable aggregates of mCherry fluorescence with no corresponding SEpH fluorescence. Posterior MTs are uniform in diameter with no morphologically distinct segments. Scale bar = 50 µm. Please click here to view a larger version of this figure.

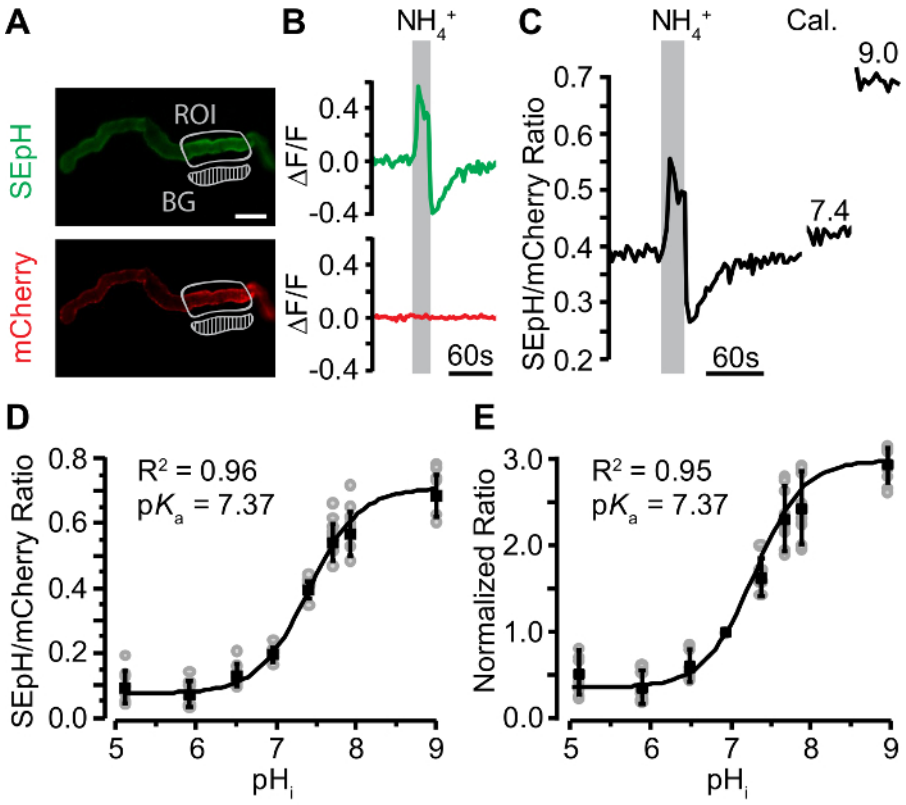

Figure 5: Validation and Calibration of pHerry in Malpighian Tubules.
A. Representative widefield images of the SEpH (470/510 nm ex/em) and mCherry (556/630 nm ex/em) components of *UAS-pHerry* driven by *capaR-GAL4* depicting healthy anterior MTs. "ROI" marks signal region of interest. "BG" marks background region of interest which was subsequently subtracted from the signal ROI in the same channel. Scale bar = 50 µm. **B**. Relative fluorescence changes in SEpH and mCherry signals of pHerry in response to a 20 s 40 mM NH_4Cl pulse. Note that the mCherry signal is stable while the SEpH signal displays a characteristic increase during the pulse (indicative of alkalization, *i.e.* increased pH_i) and a sharp decrease upon washout (indicative of acidification, *i.e.* decreased pH_i). **C**. Fluorescence ratio of pHerry (SEpH/mCherry) calculated from data in B with additional data after 30 min incubation in Calibration iPBS (10 µM nigericin, 130 mM K^+, pH 7.4 and 9.0). **D**. Calibration curve constructed from absolute pHerry ratio (SEpH / mCherry) as a function of imposed pH_i during exposure to Calibration iPBS buffered to one of eight pH values. Gray circles are individual values form 8 preparations. Black squares and bars are mean ±SD. Curve is Boltzmann fit. **E**. Same data as in D normalized such that fluorescence ratio at pH 7.0 is 1.0. Curve is modified sigmoidal curve fit (see step 7.4, **Equation 1**). Please click here to view a larger version of this figure.

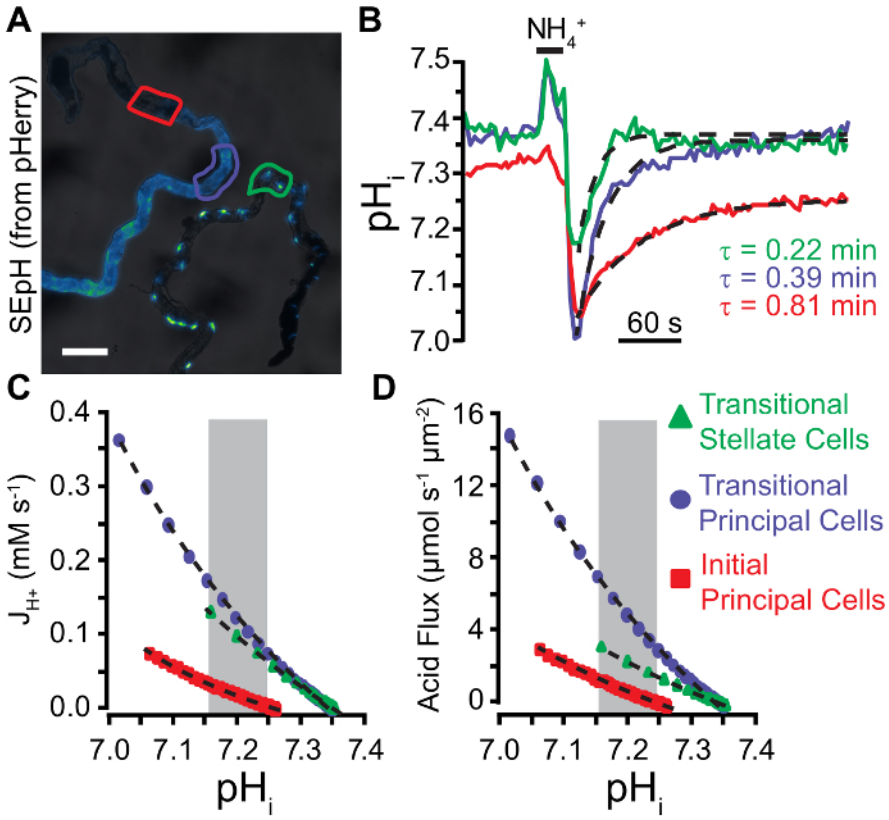

Figure 6: Quantification of Acid Extrusion in Malpighian Tubule Epithelia.
A. Widefield image of SEpH fluorescence (from pHerry) in principal cells of the anterior MT (left, driven by *capaR-GAL4* driver) and stellate cells of the anterior MT (right, driven by *c724-GAL4*). Note that stellate cells are bar-shaped in the initial segment, variable in the transitional segment, and display distinct cellular projections in the main segment. Scale bar = 100 µm. **B**. Calibrated pH_i changes in response to a 20 s 40 mM NH_4Cl pulse in the regions of interest denoted in A (principal cells of the transitional segment, principal cells of the initial segment, and stellate cells of the transitional segment). Dashed curves denote single exponential fits applied to the acid recovery phase following NH_4Cl withdrawal from which stated decay constant (τ) values are derived. **C**. Acid extrusion rate (J_{H+}) plotted as a function pH_i derived from the exponential fits seen in B. See step 8.3.1 for J_{H+} calculation (**Equation 3**). Dashed curves are exponential fits applied to each data plot within the area of overlapping pH_i denoted by the gray box. **D**. Acid flux plotted as a function pH_i derived from the exponential fits seen in B and **Equation 5**. Dashed curves are exponential fits applied to each data plot within the area of overlapping pH_i denoted by the gray box. Please click here to view a larger version of this figure.

	iPBS	NH_4Cl Pulse iPBS	Calibration iPBS
NaCl	121.5	81.5	0
NH_4Cl	0	40	0
KCl	20	20	130
Glucose	20	20	20
Buffer	HEPES; 8.6	HEPES; 8.6	MES, HEPES, or TAPS; 8.6
$NaHCO_3$	10.24	10.24	0
NaH_2PO_4 ($1H_2O$)	4.5	4.5	0
NMDG	0	0	30.5
pH	6.8	6.8	Varies
Osmolarity	350 ±5	350 ±5	350 ±5

Table 1: Experimental Fly Solutions.
iPBS solutions are prepared at room temperature and pH is set by titration with HCl and NaOH. Calibration solution is titrated with HCl and NMDG. Buffer of calibration solution is varied based on desired pH [2-(N-morpholino)ethanesulfonic acid (MES) for pH = 4.0 - 6.0; 4-(2-hydroxyethyl)-1-piperazineethanesulfonic acid (HEPES) for pH = 6.5 - 7.5; N-[tris(hydroxymethyl)methyl]-3-aminopropanesulfonic acid (TAPS) for pH = 8.0 - 9.0]. All values in mM, except pH (unitless) and osmolality (mmol/kg). Stock nigericin in DMSO is added to calibration solutions to a final concentration of 10 µM just before use.

GEpHI	Excitation (nm)	Emission (nm)	pK_a	Notes
Superecliptic pHluorin (SEpH)[11]	395, 488	530	7.2	Large linear range, large fold (50x) increase in pH-sensitive fluorescence across linear range
Pt GFP[42]	390, 475	540	7.3	Validated for use in plant cells
Superecliptic pHluorin - mCherry fusion[31]	488, 556	530, 620	7.2	Produces unpaired mCherry aggregates in some cells
ClopHensor[40]	488, 545	525, 590	6.8	pH and Cl^- sensor. Updated ClopHensorN[30] varient shows less aggregation in neurons
pHerry[10]	488, 556	530, 620	7.2	Updated SEpH-mCherry fusion with linker from ClopHensor
mNectarine[44]	558	578	6.9	Correction for photobleaching is often necessary
pHluorin2[45]	395, 475	509	6.9	Variant of Ratiometric pHluorin[12]
pHred[47]	440, 585	610	7.8	Updated varient of long-Stokes shift mKeima[49], compatible with FLIM NIR 2-photon imaging
pHuji[43]	566	598	7.7	Varient of mApple; lower than expected pH sensitivity in some cells
pHtomato[46]	550	580	7.8	Validated to track vesicular endocytosis, poor cytocolic pH sensitivity
pHoran4[43]	547	561	7.5	Enhanced pH-sensitive orange fluorescent protein
SypHer-2[48]	427, 504	525	8.1	Brighter variant of ratiometric SypHer[51], originally for mitochondrial measurements

Table 2: List of Published Cytosolic GEpHIs
Excitation maxima, emission maxima, and apparent pK_a values are approximate and can vary depending on expression system, imaging technique, and calibration method. FLIM = fluorescence lifetime imaging microscopy. NIR = near infrared.

Discussion

The success of quantification of pH_i in *Drosophila* MTs depends entirely on the health of extracted MTs and the quality of mounting and dissection (**Figure A - C**). Thus, the careful handling of tissue as described is imperative. Slides freshly coated in PLL substantially aid MT mounting as they tend to be much more adhesive than slides which have previously been exposed to solution. Careful mounting will also aid in identification of distinct MT segments (**Figure D**). Healthy MTs facilitate calibration of pHerry and functional assessment by reducing mCherry aggregation and yielding much more consistent quantification of acid extrusion, respectively. In some cases, avoiding mCherry aggregation is not possible as the experimental conditions may inherently damage MT epithelia or produce significant over-expression of the fluorescent reporter. In these cases, a pseudo-ratiometric calibration normalized such that fluorescence ratio 1.0 corresponds to pH_i 7.0, and point calibrations will permit quantification (**Figure E**). Care should be taken when performing point calibrations to avoid exposing the permanent elements of the imaging and perfusion systems to nigericin as the ionophore will adhere to glass and plastic. Even pseudo-ratiometric calibration is not possible for circumstances in which an experimental manipulation induces cellular damage during an experiment, *i.e.* this damage will cause a progressive apparent increase in mCherry fluorescence throughout the experiment. In these later cases, the SEpH fluorescence signal can be used with a normalized calibration curve and point calibrations, with the caveat that the imaging will no longer correct for movement artifacts and focal shifts.

GEpHIs carry several general limitations when compared to quantification of pH_i with fluorescent dyes. Dye retention can be used as an indicator of membrane integrity and cell health[39], but no equivalent assay is available for GEpHIs use. As such, the preparation health must

be monitored through independent means if cell damage is predicted to confound results. GEpHIs potentially permit imaging from minimally disturbed *in vivo* preparations but tissue integrity inherently limits experimental manipulations and can make point calibrations impossible. Another specific limitation inherent in using pHerry and other cytosolic dual fluorophore pH indicators (such as ClopHensor[40]) derives from the tendency of the two fluorophores to alter their fluorescence independently of both one another and pH_i. RFP aggregation artifacts are the most significant manifestation of this limitation, but quantification can also be compromised by photobleaching of one or both fluorophores. Thus, imaging protocols much be adjusted to minimize photobleaching, which can lead to long exposure times and acquisition rates <0.2 Hz. Long exposure times will fail to report rapid pH_i shifts. SEpH fluorescence shows linear correlation to pH_i from pH 6.8 - 7.8 in most preparations, but the accuracy of such measurements depends on the accuracy of the nigericin/high K^+ technique. Nigericin acts as a K^+/H^+ ionophore and proper calibration relies on equilibrating extracellular [K^+] with intracellular [K^+]. Estimates of intracellular [K^+] are not available or readily obtainable for all experimental systems. Accuracy of pH_i quantification will only be as reliable as estimates of intracellular [K^+], although rates of relative change in pH_i will be consistent. Given this limitation and the inverse logarithmic relationship of pH_i to intracellular [H^+], it is always preferable to report data as rates of change in pH_i, acid extrusion rate (J_{H+}, **Figure 6C**), or acid flux (**Figure 6D**) rather than absolute changes in pH_i. Analysis of data as acid flux has the added benefit of correcting for differences in surface are to volume ratio between cell types.

Several caveats must be appreciated when interpreting data from the adult fly MT preparation described in this protocol. The morphological distinction of the initial, transitional, and main segments is likely a simplification of the true diversity of functional and genetic domains present in the MTs[2]. Furthermore, while this protocol is designed to detect function of basolateral acid transporters it is possible that apical transport can influence pH_i measurements as well. Sealing the ureters when mounting the MTs (step 5.9) ensures that solution exchange primarily occurs at the basolateral surface but para-cellular and apical movement of ions may still influence pH_i as basolateral transport ultimately alters the cytoplasmic side of lumen/cytosolic ion gradients. Absolute separation of apical and basolateral function can be accomplished by independently perfusing the luminal and basolateral surfaces of the MT but such methods are substantially more technically demanding as they require micropipette cannulation[41].

GEpHIs present many advantages over conventional methods of measuring pH_i, and these strengths are amplified when combined with the genetic malleability and low cost of the *Drosophila* MT preparation. Quantification of pH_i has historically relied upon fluorescent dyes such as (2',7'-Bis-(2-Carboxyethyl)-5-(and-6)-Carboxyfluorescein (BCECF)[22] or complicated electrophysiological assessment via ion-selective electrodes[20,21]. As pHerry is genetically encoded, it can be expressed in specific cellular populations by specific promoters (as demonstrated here in principal cells and stellate cells of the MT, **Figure 6**) and is amenable to use in any tissue subject to transgenesis, transfection, or viral-mediated infection. Dyes are limited by cost of individual preparations and potentially complicated application protocols which convey no cell specificity in heterogeneous tissues. Ion-selective electrodes require specialized equipment for fabrication and measurement, while pHerry requires only widefield epifluorescent microscopy with conventional GFP and RFP filter sets. Use of dyes and electrodes necessitate physical as well as optical access to the tissue of interest while GEpHIs can be monitored in freshly extracted tissues and over time *in vivo*. The opportunity for live imaging in intact preparations is of particular interest when assessing the cellular physiology of pH_i regulation as no other technology permits quantification of pH_i in the presence of endogenous buffering mechanisms.

The *Drosophila* adult MT preparation presents many attractive features for those interested in cellular pH regulation and ion transport. *Drosophila* husbandry is inexpensive and tools such as genetically-encoded biosensor constructs and RNAi expression inserts are readily available from a variety of stock centers (Bloomington *Drosophila* Stock Center at Indiana University; Vienna *Drosophila* Research Center). *Drosophila* MTs are composed of a single layer of polarized epithelial cells, making them ideal for investigation of transepithelial ion transport. Basolateral transport can be easily assayed (as demonstrated here) but full assessment of apical and basolateral ion movement is possible with micropipette cannulation[41]. Additionally, organ function assays such as the Ramsay secretion assay[17] and the luminal calcium-oxalate deposition[18] are well-characterized and allow correlation of epithelial cellular physiology to models of fluid secretion and nephrolithiasis, respectively. While these features provide opportunities for robust analysis, the low-cost and wide availability of epifluorescent microscopy makes the *Drosophila* MT model ideal for demonstrations of cellular and whole-organ physiology in teaching laboratories.

Mastery of these methods permits quantification of pH_i regulation by basolateral H^+ flux in adult *Drosophila* MTs, an accessible yet robust model of transepithelial ion transport. Use of GEpHIs such as pHerry can be easily adapted to assess pH_i regulation in other invertebrate cell types, cultured mammalian cells, and *in vivo* preparations. Development of new GEpHIs will likely follow that of genetically-encoded calcium indicators, with new generations spanning the visible spectrum and addressing current limitations such as aggregation artifacts[30,42,43,44,45,46,47,48,49]. GEpHIs have already been used extensively to report mitochondrial matrix pH[50,51], and subcellular targeting strategies exist to localize biosensors to endoplasmic reticulum[52], nucleus[53], synaptic vesicles[12,43], and the cytoplasmic[54] and external surfaces of cellular plasma membrane[55] (see **Table 2** for a list of published reagents). As such tools become available they will permit vertical integration of sub-cellular pH regulation with other aspects of cellular physiology, such as Ca^{2+} handling and intracellular signaling, and whole organ function across a variety of vertebrate and invertebrate preparations.

Disclosures

The authors have nothing to disclose.

Acknowledgements

This work was supported by NIH DK092408 and DK100227 to MFR. AJR was supported by T32-DK007013. The authors wish to thank Dr. Julian A.T. Dow for the CapaR-GAL4 and c724-GAL4 *Drosophila* stocks. We also thank Jacob B. Anderson for assistance maintaining experimental fly crosses.

References

1. Dow, J. A. T., Romero, M. F. Drosophila provides rapid modeling of renal development, function, and disease. *Am J Physiol Renal Physiol.* **299** (6), F1237-F1244 (2010).
2. Sozen, M. A., Armstrong, J. D., Yang, M., Kaiser, K., Dow, J. A. Functional domains are specified to single-cell resolution in a Drosophila epithelium. *P Natl Acad Sci USA.* **94** (10), 5207-5212 (1997).
3. Davies, S. A., *et al.* Analysis and inactivation of vha55, the gene encoding the vacuolar ATPase B-subunit in Drosophila melanogaster reveals a larval lethal phenotype. *J Biol Chem.* **271** (48), 30677-30684 (1996).
4. Torrie, L. S., *et al.* Resolution of the insect ouabain paradox. *P Natl Acad Sci USA.* **101** (37), 13689-13693 (2004).
5. Evans, J. M., Allan, A. K., Davies, S. A., Dow, J. A. Sulphonylurea sensitivity and enriched expression implicate inward rectifier K+ channels in Drosophila melanogaster renal function. *J Exp Biol.* **208** (Pt 19), 3771-3783 (2005).
6. Sciortino, C. M., Shrode, L. D., Fletcher, B. R., Harte, P. J., Romero, M. F. Localization of endogenous and recombinant Na(+)-driven anion exchanger protein NDAE1 from Drosophila melanogaster. *Am J Physiol Cell Physiol.* **281** (2), C449-463 (2001).
7. Ianowski, J. P., O'Donnell, M. J. Basolateral ion transport mechanisms during fluid secretion by Drosophila Malpighian tubules: Na+ recycling, Na+:K+:2Cl- cotransport and Cl- conductance. *J Exp Biol.* **207** (Pt 15), 2599-2609 (2004).
8. O'Donnell, M. J., *et al.* Hormonally controlled chloride movement across Drosophila tubules is via ion channels in stellate cells. *Am J Physiol.* **274** (4 Pt 2), R1039-1049 (1998).
9. Cabrero, P., *et al.* Chloride channels in stellate cells are essential for uniquely high secretion rates in neuropeptide-stimulated Drosophila diuresis. *P Natl Acad Sci USA.* **111** (39), 14301-14306 (2014).
10. Rossano, A. J., Kato, A., Minard, K. I., Romero, M. F., Macleod, G. T. Na+ /H+ -exchange via the Drosophila vesicular glutamate transporter (DVGLUT) mediates activity-induced acid efflux from presynaptic terminals. *J Physiol.* **595** (3), 805-824 (2017).
11. Sankaranarayanan, S., De Angelis, D., Rothman, J. E., Ryan, T. A. The use of pHluorins for optical measurements of presynaptic activity. *Biophys J.* **79** (4), 2199-2208 (2000).
12. Miesenbock, G., De Angelis, D. A., Rothman, J. E. Visualizing secretion and synaptic transmission with pH-sensitive green fluorescent proteins. *Nature.* **394** (6689), 192-195 (1998).
13. Shaner, N. C., *et al.* Improved monomeric red, orange and yellow fluorescent proteins derived from Discosoma sp. red fluorescent protein. *Nat biotechnol.* **22** (12), 1567-1572 (2004).
14. Thomas, J. A., Buchsbaum, R. N., Zimniak, A., Racker, E. Intracellular pH measurements in Ehrlich ascites tumor cells utilizing spectroscopic probes generated in situ. *Biochemistry.* **18** (11), 2210-2218 (1979).
15. Brand, A. H., Perrimon, N. Targeted gene expression as a means of altering cell fates and generating dominant phenotypes. *Development.* **118** (2), 401-415 (1993).
16. Dietzl, G., *et al.* A genome-wide transgenic RNAi library for conditional gene inactivation in Drosophila. *Nature.* **448** (7150), 151-U151 (2007).
17. Dow, J. A., *et al.* The malpighian tubules of Drosophila melanogaster: a novel phenotype for studies of fluid secretion and its control. *J Exp Biol.* **197** 421-428 (1994).
18. Hirata, T., *et al.* In vivo Drosophilia genetic model for calcium oxalate nephrolithiasis. *Am J Physiol Renal Physiol.* **303** (11), F1555-1562 (2012).
19. Schellinger, J. N., Rodan, A. R. Use of the Ramsay Assay to Measure Fluid Secretion and Ion Flux Rates in the Drosophila melanogaster Malpighian Tubule. *J Vis Exp.* (105) (2015).
20. Caldwell, P. C. An investigation of the intracellular pH of crab muscle fibres by means of micro-glass and micro-tungsten electrodes. *J Physiol.* **126** (1), 169-180 (1954).
21. Boron, W. F., De Weer, P. Intracellular pH transients in squid giant axons caused by CO2, NH3, and metabolic inhibitors. *J Gen Physiol.* **67** (1), 91-112 (1976).
22. Rink, T. J., Tsien, R. Y., Pozzan, T. Cytoplasmic pH and free Mg2+ in lymphocytes. *J Cell Biol.* **95** (1), 189-196 (1982).
23. Bizzarri, R., Serresi, M., Luin, S., Beltram, F. Green fluorescent protein based pH indicators for in vivo use: a review. *Anal Bioanal Chem.* **393** (4), 1107-1122 (2009).
24. Kneen, M., Farinas, J., Li, Y., Verkman, A. S. Green fluorescent protein as a noninvasive intracellular pH indicator. *Biophys J.* **74** (3), 1591-1599 (1998).
25. Raimondo, J. V., Irkle, A., Wefelmeyer, W., Newey, S. E., Akerman, C. J. Genetically encoded proton sensors reveal activity-dependent pH changes in neurons. *Front Mol Neurosci.* **5** 68 (2012).
26. Raimondo, J. V., *et al.* Tight Coupling of Astrocyte pH Dynamics to Epileptiform Activity Revealed by Genetically Encoded pH Sensors. *J Neurosci.* **36** (26), 7002-7013 (2016).
27. Bagar, T., Altenbach, K., Read, N. D., Bencina, M. Live-Cell imaging and measurement of intracellular pH in filamentous fungi using a genetically encoded ratiometric probe. *Eukaryot Cell.* **8** (5), 703-712 (2009).
28. Gjetting, K. S., Ytting, C. K., Schulz, A., Fuglsang, A. T. Live imaging of intra- and extracellular pH in plants using pHusion, a novel genetically encoded biosensor. *J Exp Bot.* **63** (8), 3207-3218 (2012).
29. Greenspan, R. J. *Fly pushing: the theory and practice of Drosophila genetics.* 2nd edn, Cold Spring Harbor Laboratory Press. (2004).
30. Raimondo, J. V., *et al.* A genetically-encoded chloride and pH sensor for dissociating ion dynamics in the nervous system. *Front Cell Neurosci.* **7** 202 (2013).
31. Koivusalo, M., *et al.* Amiloride inhibits macropinocytosis by lowering submembranous pH and preventing Rac1 and Cdc42 signaling. *J Cell Biol.* **188** (4), 547-563 (2010).
32. Terhzaz, S., *et al.* Mechanism and function of Drosophila capa GPCR: a desiccation stress-responsive receptor with functional homology to human neuromedinU receptor. *PloS one.* **7** (1), e29897 (2012).
33. Boyarsky, G., Ganz, M. B., Sterzel, R. B., Boron, W. F. pH regulation in single glomerular mesangial cells. I. Acid extrusion in absence and presence of HCO3. *Am J Physiol.* **255** (6 Pt 1), C844-856 (1988).
34. Chesler, M. The regulation and modulation of pH in the nervous system. *Prog Neurobiol.* **34** (5), 401-427 (1990).
35. Rossano, A. J., Chouhan, A. K., Macleod, G. T. Genetically encoded pH-indicators reveal activity-dependent cytosolic acidification of Drosophila motor nerve termini in vivo. *J Physiol.* **591** (7), 1691-1706 (2013).

36. Roos, A., Boron, W. F. Intracellular pH. *Physiol Rev.* **61** (2), 296-434 (1981).
37. Vaughan-Jones, R. D., Wu, M. L. pH dependence of intrinsic H+ buffering power in the sheep cardiac Purkinje fibre. *J Physiol.* **425** 429-448 (1990).
38. Buckler, K. J., Vaughan-Jones, R. D., Peers, C., Nye, P. C. Intracellular pH and its regulation in isolated type I carotid body cells of the neonatal rat. *J Physiol.* **436** 107-129 (1991).
39. Bevensee, M. O., Schwiening, C. J., Boron, W. F. Use of BCECF and propidium iodide to assess membrane integrity of acutely isolated CA1 neurons from rat hippocampus. *J Neurosci Methods.* **58** (1-2), 61-75 (1995).
40. Arosio, D., *et al.* Simultaneous intracellular chloride and pH measurements using a GFP-based sensor. *Nat Methods.* **7** (7), 516-518 (2010).
41. Wu, Y., Baum, M., Huang, C. L., Rodan, A. R. Two inwardly rectifying potassium channels, Irk1 and Irk2, play redundant roles in Drosophila renal tubule function. *Am J Physiol Regul Integr Comp Physiol.* **309** (7), R747-756 (2015).
42. Schulte, A., Lorenzen, I., Bottcher, M., Plieth, C. A novel fluorescent pH probe for expression in plants. *Plant Methods.* **2** 7 (2006).
43. Shen, Y., Rosendale, M., Campbell, R. E., Perrais, D. pHuji, a pH-sensitive red fluorescent protein for imaging of exo- and endocytosis. *J Cell Biol.* **207** (3), 419-432 (2014).
44. Johnson, D. E., *et al.* Red fluorescent protein pH biosensor to detect concentrative nucleoside transport. *J Biol Chem.* **284** (31), 20499-20511 (2009).
45. Mahon, M. J. pHluorin2: an enhanced, ratiometric, pH-sensitive green florescent protein. *Adv Biosci Biotechnol.* **2** (3), 132-137 (2011).
46. Li, Y., Tsien, R. W. pHTomato, a red, genetically encoded indicator that enables multiplex interrogation of synaptic activity. *Nat Neurosci.* **15** (7), 1047-1053 (2012).
47. Tantama, M., Hung, Y. P., Yellen, G. Imaging intracellular pH in live cells with a genetically encoded red fluorescent protein sensor. *J Am Chem Soc.* **133** (26), 10034-10037 (2011).
48. Matlashov, M. E., *et al.* Fluorescent ratiometric pH indicator SypHer2: Applications in neuroscience and regenerative biology. *Biochimica et biophysica acta.* **1850** (11), 2318-2328 (2015).
49. Kogure, T., *et al.* A fluorescent variant of a protein from the stony coral Montipora facilitates dual-color single-laser fluorescence cross-correlation spectroscopy. *Nat biotechnol.* **24** (5), 577-581 (2006).
50. Llopis, J., McCaffery, J. M., Miyawaki, A., Farquhar, M. G., Tsien, R. Y. Measurement of cytosolic, mitochondrial, and Golgi pH in single living cells with green fluorescent proteins. *P Natl Acad Sci USA.* **95** (12), 6803-6808 (1998).
51. Poburko, D., Santo-Domingo, J., Demaurex, N. Dynamic regulation of the mitochondrial proton gradient during cytosolic calcium elevations. *J Biol Chem.* **286** (13), 11672-11684 (2011).
52. Stornaiuolo, M., *et al.* KDEL and KKXX retrieval signals appended to the same reporter protein determine different trafficking between endoplasmic reticulum, intermediate compartment, and Golgi complex. *Mol Biol Cell.* **14** (3), 889-902 (2003).
53. Makkerh, J. P., Dingwall, C., Laskey, R. A. Comparative mutagenesis of nuclear localization signals reveals the importance of neutral and acidic amino acids. *Curr Biol.* **6** (8), 1025-1027 (1996).
54. Zacharias, D. A., Violin, J. D., Newton, A. C., Tsien, R. Y. Partitioning of lipid-modified monomeric GFPs into membrane microdomains of live cells. *Science.* **296** (5569), 913-916 (2002).
55. McGuire, R. M., Silberg, J. J., Pereira, F. A., Raphael, R. M. Selective cell-surface labeling of the molecular motor protein prestin. *Biochem Biophys Res Comm.* **410** (1), 134-139 (2011).

